American Journal of Applied Sciences 5 (4): 340-346, 2008
ISSN 1546-9239

Effect of Stent Geometry on Phase Shift between Pressure and Flow Waveforms in Stented Human Coronary Artery

[1] Vahab Dehlaghi, [2]Siamak Najarian and [2]Mohammad Tafazzoli Shadpour
[1]Department of Medical Sciences, Kermanshah University of Medical Sciences, Kermanshah, Iran
[2]Department of Biomechanics, Faculty of Biomedical Engineering, Amirkabir University of Technology, Tehran, Iran

Abstract: Shear stress is known to play a central role in restenosis formation and is sensitive to stent geometry. Alterations of the phase shift between pressure and flow waveform created by a different stents were studied to compare the hemodynamic effects of stent design properties on restenosis in stented human coronary artery. Blood pressure waveforms were computed in three different sites, pre-stent, middle of stented arterial segment, and post-stent regions using computational fluid dynamics. Blood flow was assumed as pulsatile, incompressible, and Newtonian flow. Rigid boundary conditions were assumed for all models. The governing Navier-Stokes equations were solved using commercial software package (Fluent V6.0.12). Stents were assumed with real structure and modeled using the commercial software package (Gambit, V2.0). The alterations of the phase shift between pressure and flow waveform created by a different stents were investigated in three major regions using commercial software package (Matlab, V7.0). It is concluded that stent geometry changes the phase shift between pressure and flow waveforms in stented human coronary artery, and wall shear stress between stent struts was sensitive to these variations. The results show that variation in the phase shift is sensitive to stent geometry.

Keywords: Stent, Phase shift, Restenosis, Coronary artery, Computational fluid dynamics

INTRODUCTION

Atherosclerosis is patchy intimal plaques (atheromas) in medium and large arteries. The plaques contain lipids, inflammatory cells, smooth muscle cells, and connective tissue. Risk factors for this disease include dyslipidemia, diabetes, cigarette smoking, family history, sedentary lifestyle, obesity, hypertension, and hemodynamic. Atherosclerosis can affect all large and medium-sized arteries, including the coronary, carotid, and cerebral arteries. It is the leading cause of morbidity and mortality in the US and in most Western countries[1, 2]. In recent years, age-related mortality attributable to atherosclerosis has been decreasing, but in 2001, coronary and cerebrovascular atherosclerosis still caused more than 650,000 deaths in the US (more than cancer and almost 6 times more than accidents). Various studies have shown that independently of systemic factors, the presence of local hemodynamic factors such as wall shear stress plays a major role in the generation, progression, and destabilization of atherosclerotic plaques[3, 4].

Advanced stages of atherosclerosis can produce severe arterial stenosis requiring clinical intervention. The primary forms of intervention include bypass grafting, balloon angioplasty, and stent deployment[5]. Intravascular stents, which are small tube-like structures, can be placed into stenotic arteries to restore blood flow perfusion to the downstream tissues. Approximately, one million patients worldwide undergo a non-surgical coronary artery interventional procedure each year[6]. Stent implantations are used in 60-80% of procedures. Intra-stent restenosis occurs in 20-30% of the cases following the procedures. The phenomenon of restenosis after endothelial damage following the stent implantation is an important parameter in stent design[7].

Neointimal proliferation (NIP), composed of smooth muscle cell proliferation and extra-cellular matrix, is one of the major mechanisms of the intra–stent restenosis[8]. Three distinct phenomena have been known to cause NIP: a) The expansion of the stent wires at the time of the implantation resulting in

Corresponding Author: Vahab Dehlaghi, Assistant Professor of Biomedical Engineering, Daneshgah Avenue, Department of Medical Sciences, Kermanshah University of Medical Sciences, Kermanshah, Iran P.O. Box 1568. Tel: (0098-831)-4274618. Fax: (0098-831)- 4276477

vascular trauma. Here, there is a possible correlation between vascular injury and neointimal hyperplasia. (b) Stent implantation might induce complex interactions between blood components and stent. The materials and the roughness of stent surface may affect the adsorption of plasma proteins. (c) The stimulation of endothelial cells by arterial wall shear stress (WSS) and flow pattern might be determinants in restenosis[9, 10].

The fluid-structure interaction between stent wires and blood flow alters WSS values, particularly between stent struts[11, 12]. The in vivo studies have confirmed that an increase in the local shear stress reduces the neointimal formation[13, 14]. Variations in the failure rates associated with different stent designs have led researchers to investigate the role of near wall flow patterns[15, 16]. Some studies in the literature have suggested a link between stent design and restenosis[17, 18, 19]. It is also clear that local blood flow patterns are affected by stent design; hence, the relationships between blood flow patterns, stent design, and the process of restenosis should be investigated thoroughly. Although it is difficult to verify conclusively such relationships without suitable in vivo studies, CFD can provide an excellent research tool to help understand these underlying issues. CFD is being employed by several researchers to explore further the nature of flow stagnation patterns on stent strut shape and spacing[20, 21, 22, 23, 24]. These studies have confirmed that the flow stagnation patterns between stent struts depend most strongly on stent strut spacing and have demonstrated that vessel wall compliance has little effect on these flow patterns.

This investigation, for the first time, presents comprehensive 3D computational fluid dynamics models to analyze the phase shift between pressure and flow waveform in stented human coronary artery, together with an analysis on the WSS values in models of stented human coronary artery with differing geometrical parameters.

MATERIALS AND METHODS

CFD modeling was applied to investigate the pulsatile flow field in the vicinity of stents placed within arterial segments in a coronary artery model. The model includes a vessel length of 2D both upstream and downstream of the stented segment. In 3D simulations, stents were modeled with real structure. We used the GAMBIT (version 2.0) software to make these models. We defined the special points on stent area and by connecting these points to each other and defining the necessary wires, the real profile for a stent strut was plotted. The requested diameter and length of stents was prepared by transferring and rotating the loops. The default stent was transferred to a vessel with the same diameter. The combination of this vessel and stent is like a vessel that a stent was implanted on it. The flow domains for the normal and stented vessels were discretized with T-grid algorithm of commercial software GAMBIT (see Figure 1).

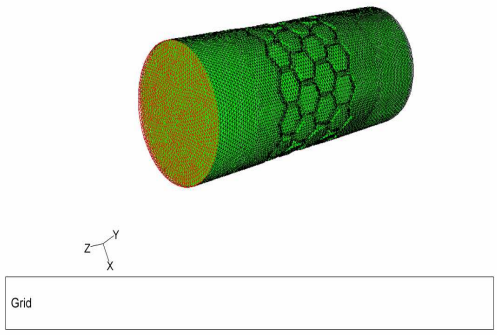

Fig. 1: The 3D stents geometry with hexagonal struts.

GAMBIT allows us to specify any volume for a meshing operation; however, the shape and topological characteristics of the volume, as well as the vertex types associated with its faces, determine the type(s) of mesh scheme(s) that can be applied to the volume. To specify the meshing scheme, one must specify two parameters: elements and type. The elements parameter defines the shape(s) of the elements that are used to mesh the volume. The type parameter defines the meshing algorithm and, therefore, the overall pattern of mesh elements in the volume. When one specifies a volume on the Mesh Volumes form, GAMBIT automatically evaluates the volume with respect to its shape, topological characteristics, and vertex types and sets the scheme option buttons to reflect a recommended volume meshing scheme. By attention to stented artery geometry, GAMBIT automatically allows us to specify the Tet/Hybrid volume meshing elements options and T-Grid volume meshing type options. Grid sensitivity tests showed a variation of less than 1% in the solution of the parameters of interest when the size of volumes decreased 10% (495,846 mesh volume increased to 545,430 mesh volume). The blood flow was modeled as an incompressible Newtonian viscous fluid governed by

Navier-Stokes equations. Taking into account the previously mentioned assumptions, the governing equations are:

$$\frac{\partial \rho}{\partial t} + \nabla \bullet (\rho U) = 0 \quad (1)$$

$$\rho \frac{DU}{Dt} = \rho \cdot g - \nabla P + \mu \nabla^2 U \quad (2)$$

where,

ρ: fluid density (kg/m^3)
U: velocity vector (m/s)
P: pressure (Pa)
g: gravity acceleration (m/s^2)
μ: fluid viscosity (Pa.s)

The outflow boundary conditions were assumed to be zero pressure at the flow outlet and no slip conditions at the vessel wall. The dynamic viscosity of blood and its density were assumed to be 3.5×10^{-3} Pa.s and 1050 kg/m^3, respectively[19, 20, 21, 22]. The blood velocity boundary conditions were obtained from phase contrast MRI scanning. Figure 2 shows the mean velocity waveforms with a 0.8 sec period that were used as the inlet velocity conditions in the computational models[25].

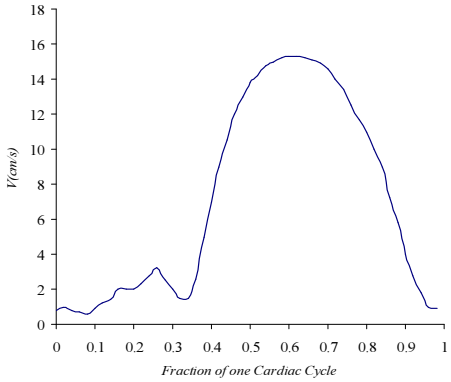

Fig. 2: Flow waveform in the inlet of coronary artery models

The Reynolds number (Re) is the ratio of inertial to viscous forces and for a circular tube is given by:

$$\mathrm{Re} = \frac{U_m D \rho}{\mu} \quad (3)$$

where,

D: characteristic length (diameter for artery)
U_m: average fluid velocity

In the case of pulsatile flow, the pulse rate was determined with the Womersley parameter, α, which represents the ratio of unsteady to viscous forces and is defined as:

$$\alpha = \frac{D}{2}\sqrt{\frac{2\pi\rho f}{\mu}} \quad (1)$$

where,

f: the frequency of the cardiac cycle (Hz)

Using the simulated flow conditions for a 2mm diameter tube, the calculated values for Womersley and Reynolds numbers were 1.53 and 100, respectively.

The commercial finite volume code FLUENT (version 6.0.12) was applied to solve the governing equations. FLUENT provides comprehensive modeling capabilities for a wide range of incompressible and compressible, laminar and turbulent fluid flow problems. In FLUENT, a broad range of mathematical models for transport phenomena (like heat transfer and chemical reactions) is combined with the ability to model complex geometries. FLUENT used a control-volume-based technique to convert the governing equations to algebraic equations that can be solved numerically. This control volume technique consists of integrating the governing equations about each control volume, yielding discrete equations that conserve each quantity on a control-volume basis.

Wall shear stress was determined as the product of viscosity and shear rate. Briefly, the Fluent flow solver calculates shear rate (γ) and shear stress (τ) during incompressible and Newtonian fluids flow using Equation (5). The accuracy of the calculation was set at 10^{-4} m/sec, which resulted in an error of WSS of less than 1%.

$$\tau = \mu \cdot \gamma$$
$$\gamma = \frac{\partial U_i}{\partial x_j} + \frac{\partial U_j}{\partial x_i} \quad (5)$$

Regions of low WSS were also expressed as percentages of the stent area within intra-strut regions in the proximal, middle and distal portions of the stent in order to determine perturbations produced by stent strut geometry. Near-wall velocity vectors were also visualized at spatial locations in the proximal, middle and distal portions of the stent to observe the behavior of blood flow in these regions.

The equation of motion of a liquid, if the pressure gradient varies with time, is:

$$\frac{\partial^2 U}{\partial r^2} + \frac{1}{r}\frac{\partial U}{\partial r} - \frac{1}{\nu}\frac{\partial U}{\partial t} = -\frac{1}{\mu}\frac{\partial P}{\partial z} \quad (6)$$

If we take the pressure difference over a distance L as the pressure gradient and represent it by a harmonic motion, then:

$$\frac{P_1 - P_2}{L} = \frac{\partial P}{\partial z} = A^* e^{i\omega t} \quad (7)$$

where ω is the frequency and the solution for the velocity, U of the lamina at a distance (y=r/R) from the axis is:

$$U(r,t) = \frac{A^*}{i\omega\rho}\{1 - \frac{J_0(\alpha y i^{3/2})}{J_0(\alpha i^{3/2})}\}e^{i\omega t}$$
$$\alpha^2 = \frac{R^2\omega\rho}{\mu} = \frac{R^2\omega}{\nu} \quad (8)$$

To obtain the volume flow Q (in cm^3/s) it is necessary to integrate the velocity across the lumen of the tube:

$$Q = \frac{\pi R^2 A^*}{i\omega\rho}\{1 - \frac{2J_1(\alpha i^{3/2})}{\alpha i^{3/2} J_0(\alpha i^{3/2})}\}e^{i\omega t} \quad (9)$$

where J_0 and J_1 are Bessel functions of order zero and one, respectively. The expression in the braces was termed $[1\text{-}F_{10}]$ by Womersley. When the real part of the pressure gradient is written as M cos(ωt-φ), Equation (9) can be written as:

$$Q = \frac{\pi R^2 A^*}{\omega\rho} M[1 - F_{10}]\sin(\omega.t - \phi) \quad (10)$$

and may be calculated in this form using the real and imaginary parts of $[1\text{-}F_{10}]$.

To consider the behavior of the oscillating components of flow in an artery, the alterations of the phase shift between pressure and flow waveform (φ) created by different stents were investigated in four major regions; artery inlet, proximal, middle, and distal portions of the stent using commercial software package (Matlab, version 7.0).

The effect of inlet length conditions will be to cause a flattening of the central region of the velocity profile. The pressure gradient in the inlet length is higher for a given rate of flow than when the same flow is established. The expression for the calculation of the inlet length for oscillatory or pulsatile flow is:

$$L = 2.64\ \frac{U}{2\pi f} \quad (11)$$

where,
f: the frequency of the cardiac cycle (Hz)
U: maximum fluid velocity

RESULTS AND DISCUSSION

Figure 3 shows the relation between flow curve and pressure gradient at the same time. It can be seen that there is a phase lag (φ) of flow behind pressure. The parameter phase lag (φ) is a function of the non-dimensional constant α. As α approaches zero, the phase lag (φ) approaches zero and pressure gradient becomes M cos(ωt). In stented human coronary artery, using the simulated flow conditions for a 2mm diameter tube, the calculated values for Womersley number (α) was 1.53 and the phase lag (φ) approaches -12.56° in the artery inlet region. Note that this phase shift is due to the inertia of the fluid.

Table 1 shows the variation of the phase shift between pressure and flow waveform (φ) created by different stents in four major regions; artery inlet, proximal, middle, and distal portions of the stent. We can see that the value of the phase shift in the proximal portions of the stent approximately equals with that of the artery inlet region. However, the variation of the phase shift between pressure and flow waveform (φ) is considerable for the middle section of the stent. In the distal portion of the stent, this change decreases slowly. In Table 1, we can see that the variations of the phase shift created by stents with different geometry in four major regions are different. The maximum appears for the stent with rectangular struts and the minimum for the elliptical struts.

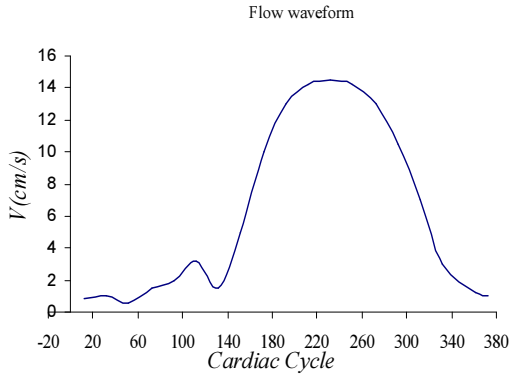

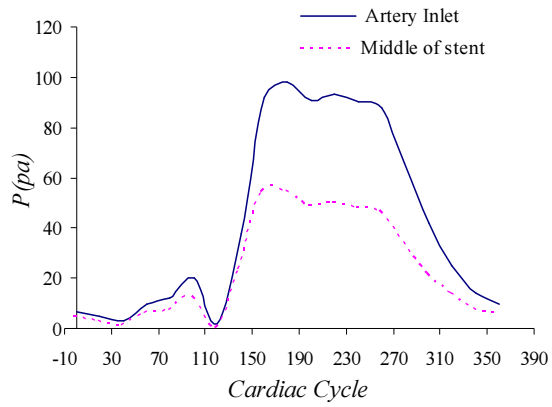

Fig. 3: Phase shift between pressure and flow waveform

Figure 4 illustrates the wall shear stress distribution in stented segment, pre-stent, and post-stent regions in 3D model of stent with rectangular strut. The results show that the presence of stents markedly affects the WSS distribution. The WSS distribution depended on the flow waveform. So, there is a phase shift between pressure gradient and WSS distribution at the same time. This phase shift equals with the phase shift between flow curve and pressure gradient at the same time. These results demonstrate that the phase lag (φ) between flow curve and WSS distributions approaches zero.

The maximum WSS in the part of vessel which is limited between the stent struts has the phase shift that differs from its value in the unstented vessel and this amount will increase during the stent length, as well. This figure shows that in the stent strut, the corners are the critical areas, i.e., areas with low wall shear stress (<12.6 dynes/cm²). They displayed a significant increase in the thickness of the atherosclerotic plaque and the vessel wall (positive remodeling). Areas with physiologic wall shear stress (12.6-26.9 dynes/cm²) did not display significant changes, and areas exposed to a high wall shear stress (≥ 27 dynes/cm²) displayed positive remodeling of the artery without changes in the atheroma plaque[3]). WSS in these locations is less than 1.26 Pa. Values of WSS in the proximal of stent are more than the distal values, so it is confirmed that the restenosis will increase in long stents.

The WSS on stent strut profiles is 2 or 2.5 times higher, and hence, it is more than its value in the vessel without stent (Figure 5).

The first and second loops of a rectangular stent struts were compared with each other in Table 2. Here, one can see the percentage of loop surface and WSS in stented vessel and unstented vessel.

Table 3 shows the effect of the flow divider on the alterations of the phase shift between pressure and flow waveform (φ) created by different stents in four major regions. The flow divider caused an increase for these alterations by more than 50% in the proximal portions, and 80% in the middle of stented segment. These alterations for rectangular, hexagonal, and elliptical stent struts are compared with each other in Table 2. The results show that these values of phase shift for rectangular, elliptical, and hexagonal struts are equal.

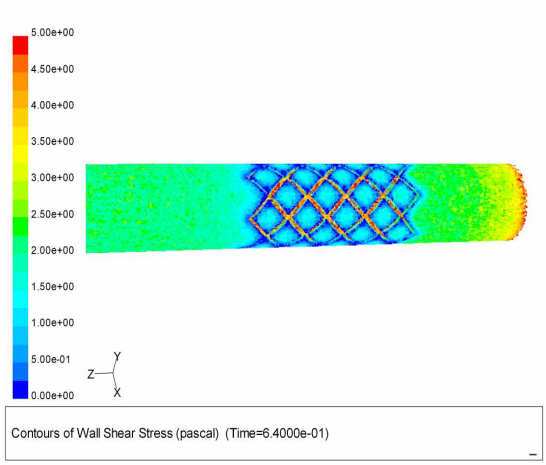

Fig. 4: Contours of *WSS* for stented coronary artery with rectangular struts in the 0.64 Sec. from cardiac cycle

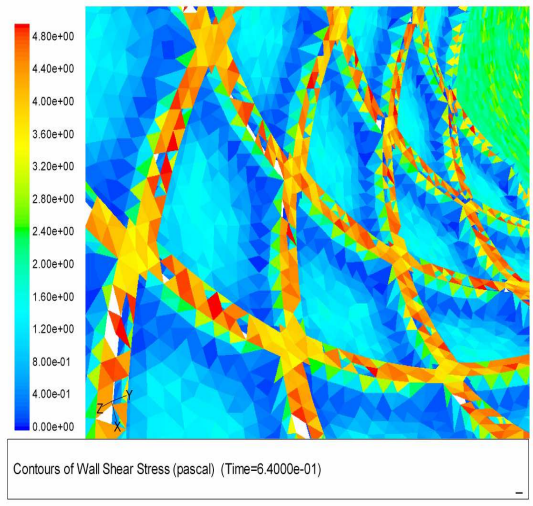

Fig. 5: Contours of *WSS* on stent strut profiles with rectangular struts in the 0.64 sec from cardiac cycle

Table 1: Phase shift between pressure and flow waveform (φ) created by different stents

Stents geometry	Artery inlet	Proximal of stent	Middle of stent	Distal of stent
Elliptical struts	-12.56	-12.68	-14.56	-14.16
Hexagonal struts	-12.56	-12.74	-14.72	-14.24
Rectangular struts	-12.56	-12.82	-15	-14.5

Table 2: *WSS* in the first and second stent struts for stented coronary artery with rectangular strut

Second strut area %	First strut area %	*WSS* (with stent)/*WSS* %
4	10	40-50
16	20	30-40
23	20	20-30
27	25	10-20
30	25	0-10

Table 3: Phase shift between pressure and flow waveform (φ) created by different stents and flow divider

Stents geometry	Artery inlet	Proximal of stent	Middle of stent	Distal of stent
Elliptical struts	-12.56	-12.75	-16.5	-16
Hexagonal struts	-12.56	-12.84	-17.2	-16.5
Rectangular struts	-12.56	-12.95	-17.8	-17

CONCLUSION

Some studies in the literature have suggested a link between stent design and restenosis. It is also clear that the local blood flow patterns are affected by stent design; hence, the relationships between blood flow patterns, stent design, and the process of restenosis was investigated thoroughly in this work.

The current results confirm and extend our previous observations and further demonstrate the importance of stent geometry on the intravascular fluid dynamics. The current findings with 3D computational fluid dynamics modeling demonstrate that there is a phase lag (φ) of flow behind pressure. This phase lag (φ) is a function of the non-dimensional constant α and stent geometry. Therefore, the parameter phase lag alters the wall shear stress distribution and growth of intimal thickening in stented segment. It can be concluded that the stent strut with elliptical geometry is more appropriate than those with hexagonal and rectangular geometry, respectively. The results show that the alterations of the phase shift between pressure and flow waveform (φ) created by different stents in four major regions were influenced by flow divider. The size of this phase shift increased with flow divider.

The current results support the hypothesis that local flow patterns created by the stent should also be considered during stent design so as to minimize the indices of fluid dynamics implicated in neointimal hyperplasia.

ACKNOWLEDGEMENTS

The authors thank Dr. N. Fatouraee and Dr. H. Niroomand Oscuii (Department of Biomechanics, Faculty of Biomedical Engineering, Amirkabir University of Technology) for their technical and computational support. We also would like to express our gratitude to the Center of Excellence of Biomedical Engineering of Iran based in Amirkabir University of technology, Faculty of Biomedical Engineering for its contribution.

REFERENCES

1. LaDisa, J.F.J., L.E. Olson, R.C. Molthen, D.A. Hettrick, P.F. Pratt, M.D. Hardel, 2005. Alterations in Wall Shear Stress Predict Sites of Neointimal Hyperplasia after Stent Implantation in Rabbit Iliac Arteries. Am. J. Physiol. Heart Circ. Physiol., 288: 2465-75.

2. Najarian, S., J. Dargahi, F. Firouzi, F. Afsari, 2006. Unsteady Simulation of Distal Blood Flow in an End-to-Side Anastomosed Coronary Bypass Graft with Stenosis. Bio-Med. Mater. and Eng., 16(5): 337-347.
3. Mongrain, R., J. Rodés-Cabau, 2006. Role of Shear Stress in Atherosclerosis and Restenosis after Coronary Stent Implantation. Rev. Esp. Cardiol., 59: 1-4.
4. Hayashi, k., Y. Yanai, T. Naiki, 1996. A 3D-LDV Study of the Relation Between Wall Shear Stress and Intimal Thickness in a Human Aortic Bifurication. ASME J. Biomech. Eng., 118: 273-279.
5. Danenberg, H.D., F.G. Welt, M. Walker, 2002. Systemic Inflammation Induced by Lipopolysaccharide Increases Neointimal Formation after Balloon and Stent Injury in Rabbits**.** Circulation, 105: 2917-2922.
6. Virmani, R., A. Farb, G. Guagliumi, F.D. Kolodgie, 2004. Drug-Eluting Stents: Caution and Concerns for Long-Term Outcome. Coronary Artery Disease, 15: 313-318.
7. Kastrati, A., J. Mehilli, J. Dirsschinger, 2001. Restenosis after Coronary Placement of Various Stent Types. Am. J. Cardiolo., 877: 34-39.
8. Wentzel, J.J., R. Krams, J.C.H. Schuurbiers, 2001. Relationship Between Neointimal Thickness and Shear Stress after Wall Stent Implantation in Human Coronary Arteries. Circulation, 103: 1740-1745.
9. Wentzel, J.J., F.J.H. Gijsen, N. Stergiopulos, 2003. Shear Stress, Vascular Remodeling and Neointimal Formation. J. Biomech., 36: 681-688.
10. Carlier, S.G., J.J. Wentzel, P.W. Serruys, R. Krams, 2003. Augmentation of Wall Shear Stress Inhibits Neointimal Hyperplasia after Stent Implantation. Circulation, 107: 2741-2746.
11. Berry, J.L., J.E. Moore, W.D. Routh, 2000. Experimental and Computational Flow Evaluation of Coronary Stents. Ann. Biomed. Eng., 28: 386-398.
12. LaDisa, J.F.J., L.E. Olson, R.C. Molthen, D.A. Hettrick, P.F. Pratt, M.D. Hardel, 2005. Circumferential Vascular Deformation after Stent Implantation Alters Wall Shear Stress Evaluated Using Time-dependent 3D Computational Fluid Dynamics Models**.** J. Appl. Physiol., 98: 947-957.
13. DePaola, N., M.A.J. Gimbrone, P.F. Davies, C.F. Dewey, 1992. Vascular Endothelium Responds to Fluid Shear Stress Gradients. Arterioscler Thromb., 12: 1254-1257.
14. Kleinstreuer, C., S. Hyun, J.R. Buchanan, P.W. Longest, J.P. Archie, G.A. Truskey, 2001. Hemodynamic Parameters and Early Intimal Thickening in Branching Blood Vessels. Crit Rev Biomed Eng., 29: 1-64.
15. Garasic, J.M., E.R. Edelman, J.C. Squire, P. Seifert, M.S. Williams, C. Rogers, 2000. Stent and Artery Geometry Determine Intimal Thickening Independent of Arterial Injury. Circulation, 101: 812-818.
16. Murata, T., T. Hiro, T. Fujii, 2002. Impact of the Cross-Sectional Geometry of the Post-Deployment Coronary Stent on In-Stent Neointimal Hyperplasia: an Intravascular Ultrasound Study. Circulation, 66: 489-493.
17. LaDisa, J.F.J., L.E. Olson, R.C. Molthen, D.A. Hettrick, P.F. Pratt, M.D. Hardel, 2004. Stent Design Properties and Deployment Ratio Influence Indexes of Wall Shear Stress: a Three-Dimensional Computational Fluid Dynamics Investigation within a Normal Artery. J. Appl. Physiol., 97: 424-430.
18. Nicoud, F., H. Vernhet, M. Dauzat, 2005. A numerical Assessment of Wall Shear Stress Changes after Endovascular Stenting. J. Biomech., 38: 2019-2027.
19. Dehlaghi, V., S. Najarian, M. Tafazzoli-Shadpour, 2007. Effect of The Flow Divider on Restenosis in Stented Human Coronary Artery. J. of Qazvin University of Medical Sciences, Accepted for publication.
20. Dehlaghi, V., M. Tafazzoli-Shadpour, 2006. Analysis of Pulsatile Blood Flow in Stented Human Coronary Arteries. Proce. of the 5th World Cong. of Biomec., Munich, Germany.
21. Dehlaghi, V., M. Tafazzoli-Shadpour, S. Najarian, 2007. Analysis of 3D and Steady Blood Flow in Stented Human Coronary Artery. Amirkabir J. Sci. Tech., Accepted for publication.
22. Dehlaghi, V., M. Tafazzoli-Shadpour, S. Najarian, 2007.Numerical Analysis of Pulsatile Blood Flow in a Stented Human Coronary Artery with a Flow Divider. Am. J. Appl. Sci., 4(6): 397-404.
23. Dehlaghi, V., S. Najarian, M. Tafazzoli-Shadpour, 2007. Analysis of Wall Shear Stress in Stented Coronary Artery Using 3D Computational Fluid Dynamics Modeling. J. Mater. Proc. Technology, Accepted for publication.
24. LaDisa, J.F.J., L.E. Olson, R.C. Molthen, D.A. Hettrick, D.C. Warltier, J.R. Kersten, P.S. Pagel, 2006. Alterations in Regional Vascular Geometry Produced by Theoretical Stent Implantation Influence Distributions of Wall Shear Stress: Analysis of a Curved Coronary Artery Using 3D Computational Fluid Dynamics Modeling. J. Biomed. Eng. Online, 5:40.
25. Suo, J., Y. Yang, J. Oshinski, A. Tannenbaum, J. Gruden, D. Gjddens, 2004. Flow Patterns and Wall Shear Stress Distributions at Atherosclerotic-Prone Sites in a Human Left Coronary Artery - An Exploration Using Combined Methods of CT and Computational Fluid Dynamics. Proc. of the 26th Ann. Inte. Conf. of the IEEE EMBS San Francisco, CA, USA, September 1-5.